

2. HEAT FLOW MEASUREMENTS IN THE WEDDELL SEA, ANTARCTICA: ODP LEG 113¹

Toshiyasu Nagao²

ABSTRACT

From January to March 1987, heat flow measurements were tried at four sites (Sites 689, 690, 695, and 696) during ODP Leg 113, in the Weddell Sea, Antarctica. At Site 690 (Maud Rise), a convex upward shaped temperature vs. depth profile was observed. This profile cannot be explained by steady-state conduction through solid materials only. We conclude that the minimum heat flow value at Site 690 is 45 mW/m². A prominent bottom simulating reflector (BSR) was observed at 600 mbsf at Site 695. However, the observed temperature is too high to explain the BSR as a gas hydrate. The origin of the BSR remains unknown, although it is probably of biogenic origin as observed in the Bering Sea during DSDP Leg 19. After correcting for the effects of sedimentation, heat flow values at Sites 695 and 696 are 69 and 63 mW/m², respectively. Furthermore, we compiled heat flow data south of 50°S. In the Weddell Sea region, the eastern part shows relatively low heat flow in comparison with the western part, with the boundary between them at about 15°W longitude.

INTRODUCTION

The Weddell Sea is at present part of the Antarctic lithospheric plate, lying between East Antarctica and the Scotia Sea and bounded on the west by the Antarctic Peninsula.

The first heat flow measurements in the Scotia and Weddell Seas were reported by Zlotnicki et al. (1980). The heat flow at five Weddell Sea locations was reported as relatively high in comparison with the heat flow vs. age relationship (Lister, 1977; Parsons and Sclater, 1977).

From December 1984 to April 1985, *Discovery* made geophysical and geological investigations along the Pacific margin of the Antarctic Peninsula and in the Weddell Sea. During the cruise, they made five heat flow measurements across the Jane Basin, and obtained heat flow values of 70 to 90 mW/m² (B. D. Vedova, pers. comm.). Their preliminary results suggested that this basin is ca. 25–30 m.y. old (Lawver et al., 1985).

In the Weddell Sea, researchers on the Japanese scientific research vessel *Hakurei* also made heat flow measurements in 1981–82 and 1987–88 Antarctic summer seasons. They obtained 11 heat flow values (Okuda et al., 1983, Yamaguchi, pers. comm.).

Figure 1 shows compilation of heat flow data south of 50°S, through 1988 (Chapman, 1983; Kimura, 1982; Sato et al., 1984; Tsumuraya et al., 1985; Mizukoshi et al., 1986; Dougherty et al., 1986; Saki et al., 1987; Yamaguchi et al., 1988). Figure 1 includes 134 independent heat flow determinations. The most important feature of heat flow distribution in the Weddell Sea is the relatively low heat flow on the eastern side and relatively high heat flow on the western side.

TEMPERATURE MEASUREMENTS

During the cruise, we drilled at nine sites, but reliable temperature measurements were made at only four sites (Sites 689, 690, 695, and 696).

In situ temperatures were measured by the Von Herzen APC (advanced piston corer) tool (Horai and Von Herzen, 1986; VH-probe) and Uyeda T-probe (Yokota et al., 1980; T-probe). The

VH-probe is inserted into the cutting shoe of the APC to record temperature where the sediment is undisturbed by drilling. The temperature record contains a disturbance due to frictional heating associated with penetration of the APC into the sediment. The equilibrium formation temperature was extrapolated from the decay curve of the disturbance according to the theory of Horai and Von Herzen (1986).

The T-probe can be housed in the pressure case of the Barnes pore-water sampler: the temperature sensor is installed in a probe at the nose of the sampler. Both T-probe and VH-probe record sediment temperature at 1-min intervals.

Site 689 (64°31.0'S, 03°06.0'E)

Site 689 is located near the crest of Maud Rise, in the Weddell Sea at a water depth of 2080 m. At this site, two temperature measurements (Cores 113-689D-3H and -6H) were made with the VH-probe. Reliable data, however, were taken only from Core 113-689D-3H at 47.0 mbsf (meters below seafloor; Fig. 2). The temperature reached 8.70°C just after penetration, because of frictional heat production, and was 5.23°C just before pull-out. The temperature gradually approximated the true formation temperature.

The temperature data obtained by the VH-probe can be extrapolated to equilibrium following Horai and Von Herzen (1986). The estimated equilibrium temperature and its standard deviation is 4.63° ± 0.11°C.

Site 690 (65°09.6'S, 1°12.3'E)

Site 690 lies on the southwestern flank of Maud Rise, in 2914 m of water, and 116 km southwest of Site 689. A temperature measurement was made with the VH-probe in Hole 690C. The device was used three times (Cores 113-690C-4H, -6H, and -9H; Figs. 3 and 4). Reliable data, however, were obtained on only two measurements (Cores 113-690C-4H and -9H, at 35.2 and 83.6 mbsf). The estimated true formation temperatures and their standard deviations are 3.29° ± 0.13°C at 35.2 mbsf and 5.08° ± 0.08°C at 83.6 mbsf.

Site 695 (62°23.5'S, 43°27.1'W)

Site 695 is located on the southeastern edge of the South Orkney microcontinent on the northern margin of the Weddell Sea in 1302 m of water depth. One of the main objectives of this site was to learn about the origin of a prominent bottom-simulating reflector (BSR), considered before drilling to represent

¹ Barker, P. F., Kennett, J. P., et al., 1990. *Proc. ODP, Sci. Results*, 113: College Station, TX (Ocean Drilling Program).

² Earthquake Research Institute, University of Tokyo 1-1-1 Yayoi, Bunkyo-ku, Tokyo 113, Japan. Present address: Faculty of Science, Kanazawa University 1-1, Marunouchi, Kanazawa 920, Japan.

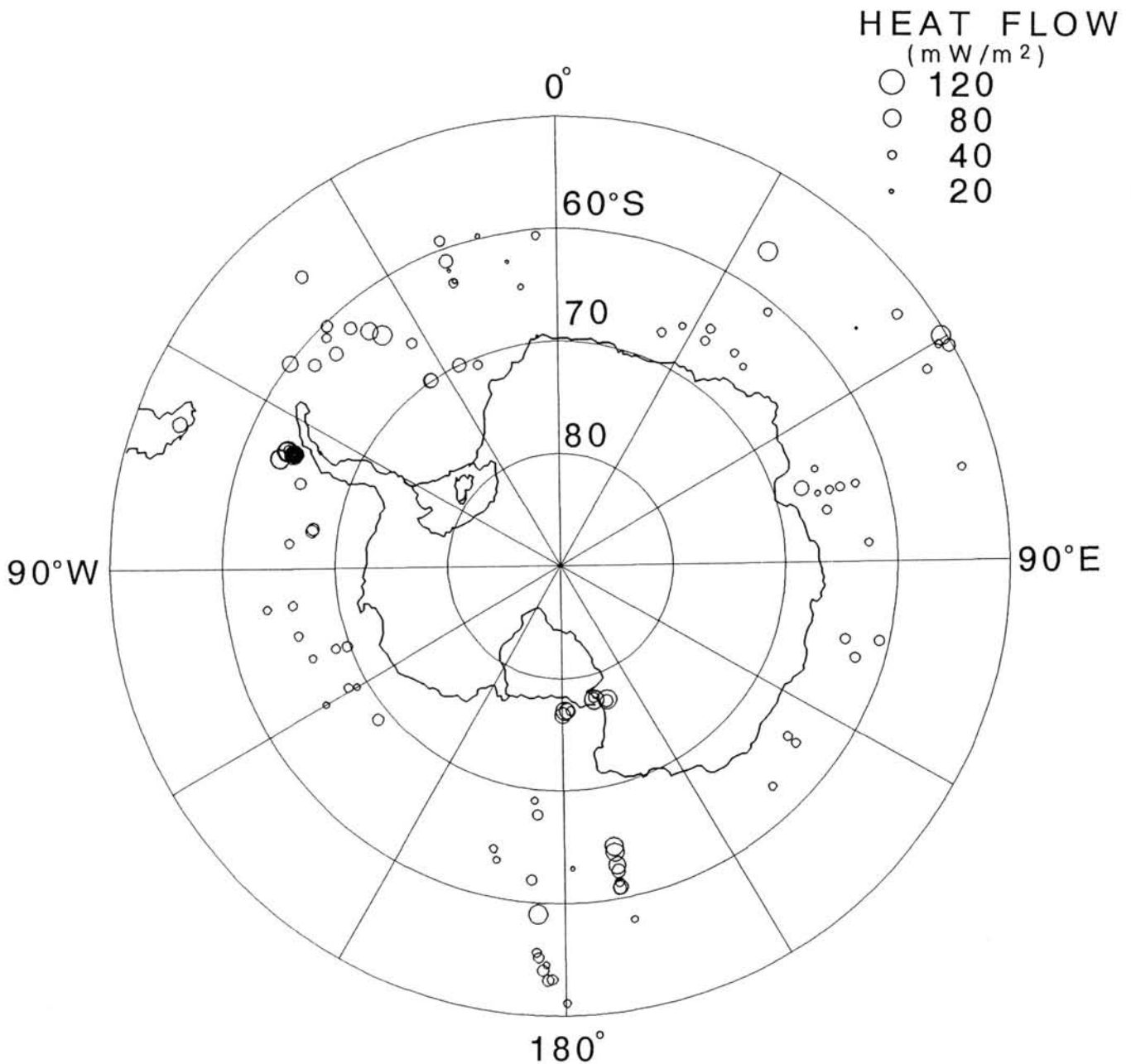


Figure 1. Compiled heat flow data south of 50°S, through 1988. The diameter of circle is proportional to the heat flow value.

the base of a gas hydrate stability zone. In this site, the VH-probe and the T-probe were used eight times (Cores 113-695A-5H, -8H, -11I, -14H, 17I, -24I, -31I and -38I). The results are described as follows:

Core 113-695A-5H (41.2 mbsf)

We used VH-probe and obtained a good result. The estimated true formation temperature and its standard deviation are $2.67^\circ \pm 0.15^\circ\text{C}$ (Fig. 5).

Core 113-695A-8H (70.0 mbsf)

We used VH-probe and the temperature reached 4.97°C just after penetration. However, the device malfunctioned, and no reliable data were obtained.

Core 113-695A-11I (89.2 mbsf)

This core was taken to obtain a pore-water sample. We used the VH-probe and the T-probe, simultaneously. Both temperature recording devices worked well. However, temperature records were somewhat unstable during the time of bottom penetration. This instability was probably produced by sensor movement as a result of ship's motion (Fig. 6).

Core 113-695A-14H (118.2 mbsf)

We used VH-probe and obtained a good result. The estimated true formation temperature and its standard deviation are $6.88^\circ \pm 0.10^\circ\text{C}$ (Fig. 7).

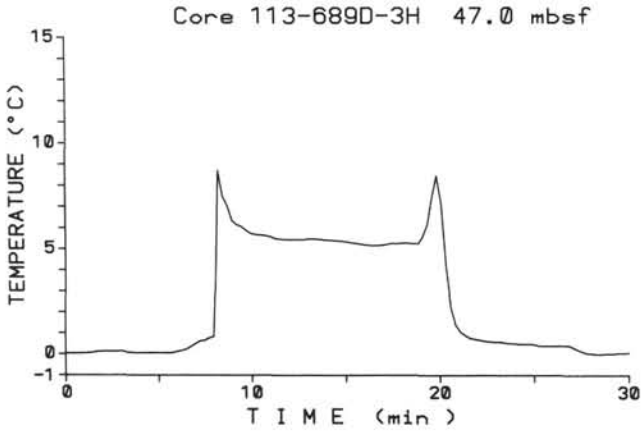


Figure 2. Temperature measurement by VH-probe on Core 113-689D-3H.

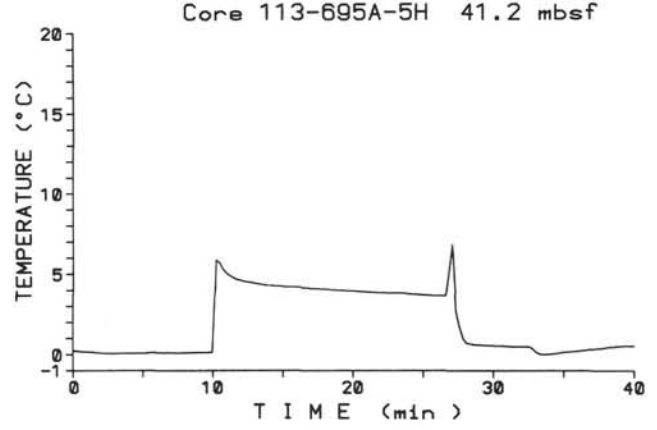


Figure 5. Temperature measurement by VH-probe on Core 113-695A-5H.

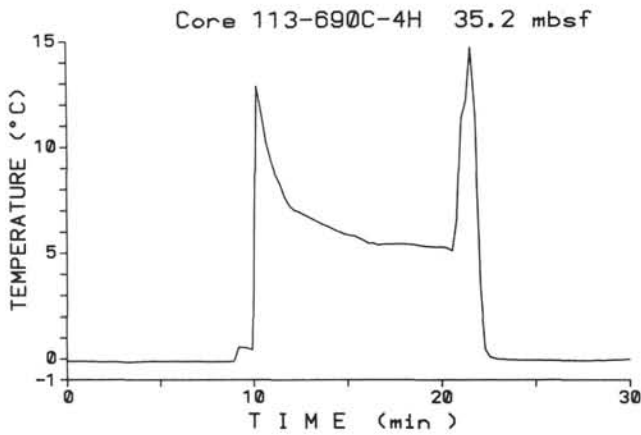


Figure 3. Temperature measurement by VH-probe on Core 113-690C-4H.

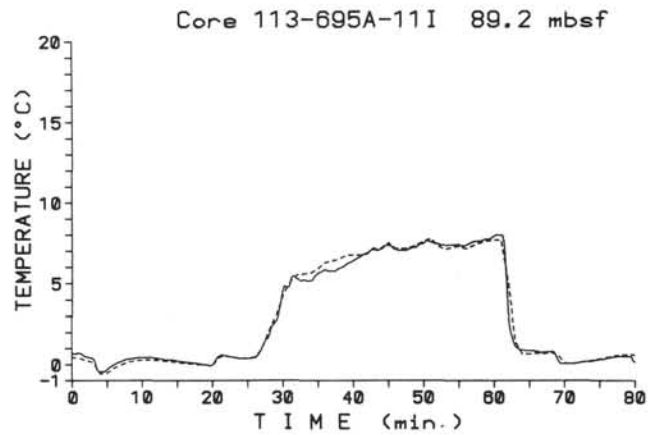


Figure 6. Temperature measurements on Core 113-695A-11I by VH-probe (solid line) and T-probe (dashed line).

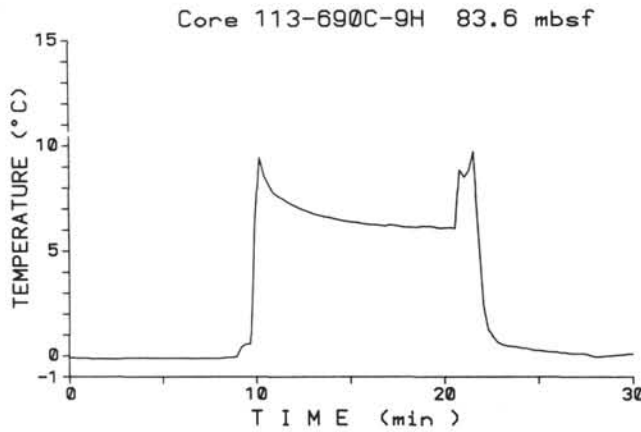


Figure 4. Temperature measurement by VH-probe on Core 113-690C-9H.

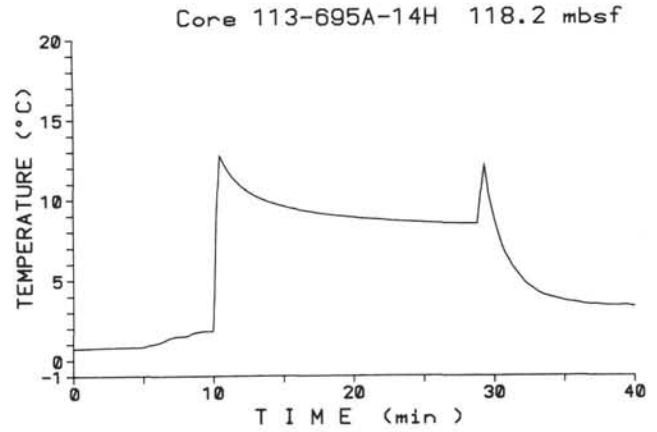


Figure 7. Temperature measurement by VH-probe on Core 113-695A-14H.

Core 113-695A-17I (137.6 mbsf)

This core was taken to obtain a pore-water sample. We used the VH-probe and the T-probe, simultaneously. However, the T-probe did not work. Just before pull-out, the VH-probe temperature was 7.21°C, and the temperature was still increasing. Thus, this provides only a minimum temperature (Fig. 8).

Core 113-695A-24I (196.6 mbsf)

We used the VH-probe and the T-probe, simultaneously. However, the T-probe did not work again. Just before pull-out, the temperature recorded by the VH-probe was 4.26°C, and the temperature was still increasing. Thus, this provides also only a minimum temperature (Fig. 9).

Core 113-695A-31I (254.4 mbsf)

The VH-probe and the T-probe were used with the pore water sampler. Both temperature recording devices worked well. Just before pull-out, VH-probe showed a temperature of 10.44°C, and was still increasing. On the other hand, the T-probe showed 15.69°C, and still decreasing (Fig. 10). This large temperature difference may be attributed to the sensor position. For pore water sampling, the *in situ* sediments were already removed by the previous coring operation. The VH-probe is located in a

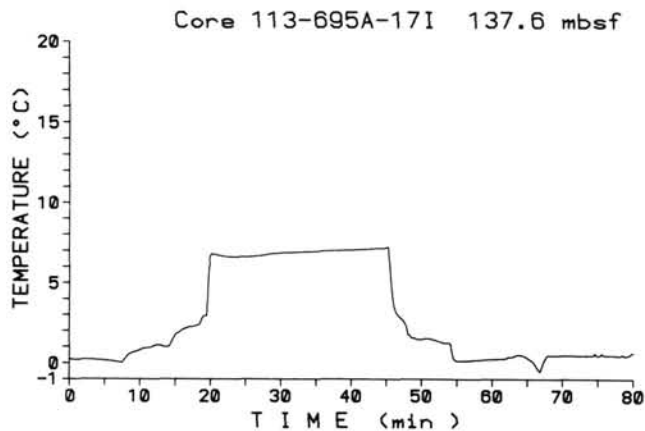


Figure 8. Temperature measurement by VH-probe on Core 113-695A-17I.

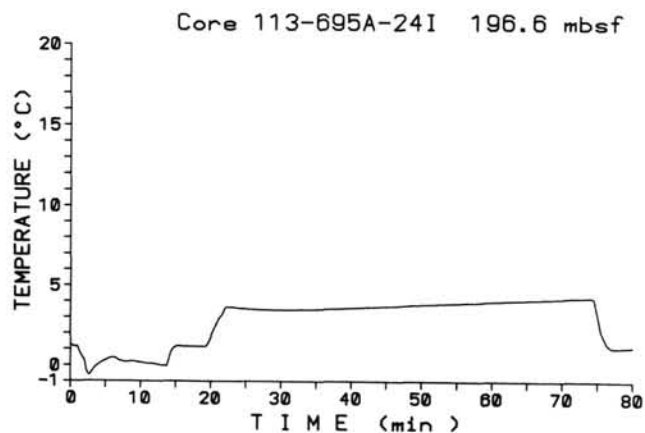


Figure 9. Temperature measurement by VH-probe on Core 113-695A-24I.

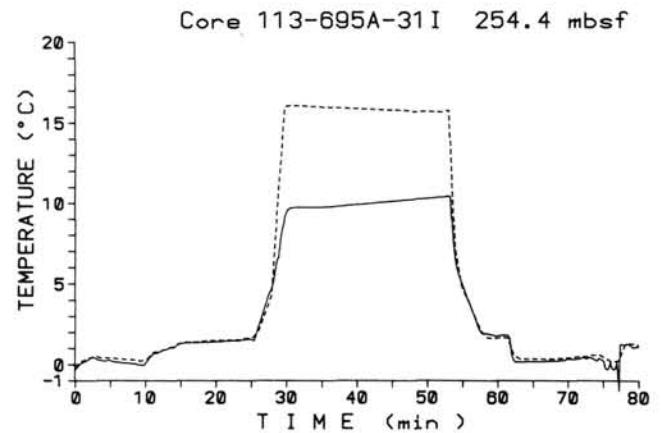


Figure 10. Temperature measurements on Core 113-695A-31I by VH-probe (solid line) and T-probe (dashed line).

wall of the APC cutting shoe. Inside the APC cutting shoe, there is probably drilling fluid, not true sediment. In contrast, the pore-water sampling needle and the sensor part of the T-probe are located 15–30 cm lower than the APC cutting shoe, and are inserted into the sediments. In this interval, the true formation temperature was between 10.44°C and 15.69°C.

Core 113-695A-38I (312.7 mbsf)

The VH-probe and the T-probe were used again and both temperature recording devices worked well. Just before pull-out, the VH-probe gave a temperature of 8.69°C, and was still increasing. The T-probe showed an almost constant temperature of 16.19°C, although it might be seen as increasing slightly. Therefore, the true formation temperature was at least and very close to 16.19°C (Fig. 11).

Site 696 (61°50.9'S, 42°56.0'S)

Site 696 is located on the southeast margin of the South Orkney microcontinent, South Scotia Ridge. In this site, the VH-probe and the T-probe were used three times (Cores 113-696A-8H, -9I, and 18I). However, reliable data were obtained for only two attempts.

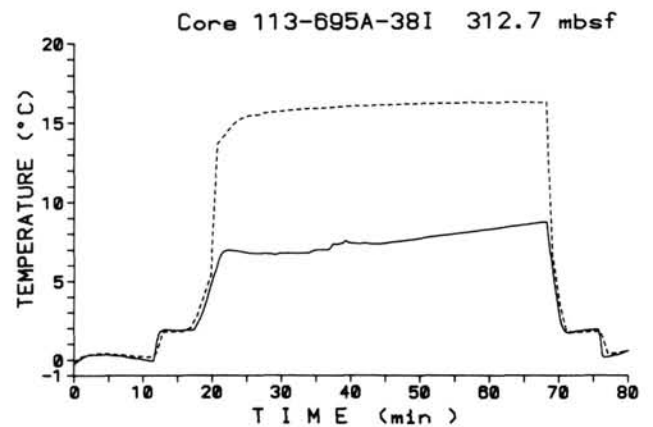


Figure 11. Temperature measurements on Core 113-695A-38I by VH-probe (solid line) and T-probe (dashed line).

Core 113-696A-8H (69.6 mbsf)

Good results were obtained using the VH-probe. The estimated true formation temperature and its standard deviation are $4.26^\circ \pm 0.10^\circ\text{C}$ (Fig. 12).

Core 113-696B-9I (144.1 mbsf)

This core was taken to obtain a pore-water sample, and we used the T-probe. Just before pull-out, the T-probe showed an almost constant, possibly slightly increasing, temperature of 7.88°C (Fig. 13).

Thermal Conductivity

The thermal conductivity of the sediment samples of Leg 113 was measured following the methods of Von Herzen and Maxwell (1959) using the needle-probe technique.

The standard sample was tested at the beginning and end of the leg. We measured one onboard standard sample, which has a recommended value of 2.25 W/m K . At the beginning of the leg, we made four measurements, and obtained a value of $2.32 \pm 0.13\text{ W/m K}$. This was 3% larger than the recommended value, but coincided within the standard deviation. We also made 20 calibration measurements at the end of the leg. This time, the measured mean conductivity of the standard sample

was $2.66 \pm 0.08\text{ W/m K}$. This is 18% higher than the recommended value.

According to previous work (Ratcliffe, 1960; Bullard and Day, 1961; Lachenbruch and Marshall, 1966), thermal conductivity and water content are strongly correlated. Figure 14 shows thermal conductivity vs. water content for Leg 113 samples. The superimposed dashed lines 1, 2, and 3 are Ratcliffe's, Bullard and Day's, and Lachenbruch and Marshall's empirical results, respectively. In Figure 14, we plotted "selected" thermal conductivity data (Table 1). "Selected" means that the thermal conductivity and water content were measured at the same position within a core. The observed thermal conductivity values are larger than those of previous workers, for the same water content. Lachenbruch and Marshall's measurements were made on Arctic Ocean floor sediments. They noted that empirical formulae based on water content underestimate sediment conductivity by 10%–20% on the rise and 5%–10% in the basin area of the Arctic Ocean. However, the observed thermal conductivity values are 15%–20% higher, for a given water content, than those of Lachenbruch and Marshall. We conclude that the observed high thermal conductivity values are mainly caused by instrument errors. At this stage, we have no idea how to correct the observed conductivities.

Thermal conductivities measured in the laboratory are usually corrected to *in situ* temperature and pressure conditions following Ratcliffe (1960). According to Morin and Von Herzen (1986), these effects never exceed 3%. However, for this leg, the calibration problem is more serious. Therefore, the temperature and the pressure corrections were not made.

Therefore, thermal conductivities obtained during the ODP Leg 113 may contain an error of +15% to +20%. This means that determined heat flow values may also be +15% to +20% too high.

DISCUSSION**Sites 689 and 690 (Maud Rise)**

At Site 690, we were able to obtain two equilibrium temperature vs. depth points as mentioned before. Furthermore, the records in the mud line showed that the temperature around the sea bottom is about 0°C . Figures 15 and 16 show observed temperatures and thermal conductivities at Sites 689 and 690. The temperature gradients in the shallower parts of both holes are similar if we assume sea bottom temperature is 0°C . However, the temperature gradient in Hole 690C does not show a linear profile but instead a convex upward shape. In Hole 690C, the temperature gradients and the averaged thermal conductivities between 0 and 35.2 mbsf, and between 35.2 and 83.6 mbsf are 93 mK/m and $1.06 \pm 0.05\text{ W/m K}$ (2 data points), and 36 mK/m and $1.25 \pm 0.11\text{ W/m K}$ (5 data points), respectively. Therefore, calculated heat flows over these two depth ranges are 99 and 45 mW/m^2 , respectively. If the heat transfer is conductive and in steady state, these values should be the same. If the basal heat flux of 45 mW/m^2 at Site 690 is true, steady-state solid conduction model suggests that the sea bottom temperature at this site should be 1.78°C . This temperature is calculated by using the lower part of temperature vs. depth relationship and thermal conductivities. From the oceanographic point of view, this 1.78°C is too high (Pudsey et al., 1988).

If this convex shape is true, several mechanisms may cause this type of nonlinear temperature profile. Four of them appear worth considering: (1) pore water convection through sediments; (2) variation of thermal conductivity with depth; (3) effects of sea bottom water temperature change; and (4) topographic effect (heat flow refraction).

The mechanism (2) could explain some, but not all, of this nonlinear profile. The mechanism (3) was also proposed by

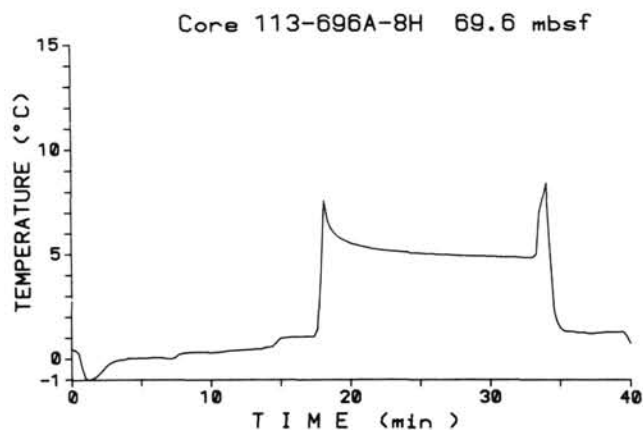


Figure 12. Temperature measurement by VH-probe on Core 113-696A-8H.

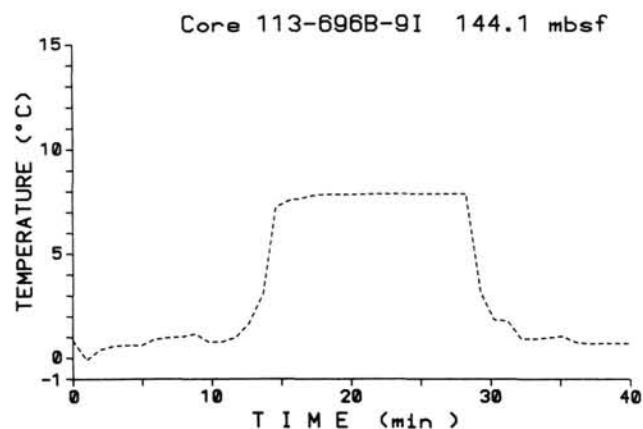


Figure 13. Temperature measurement by T-probe on Core 113-696B-9I.

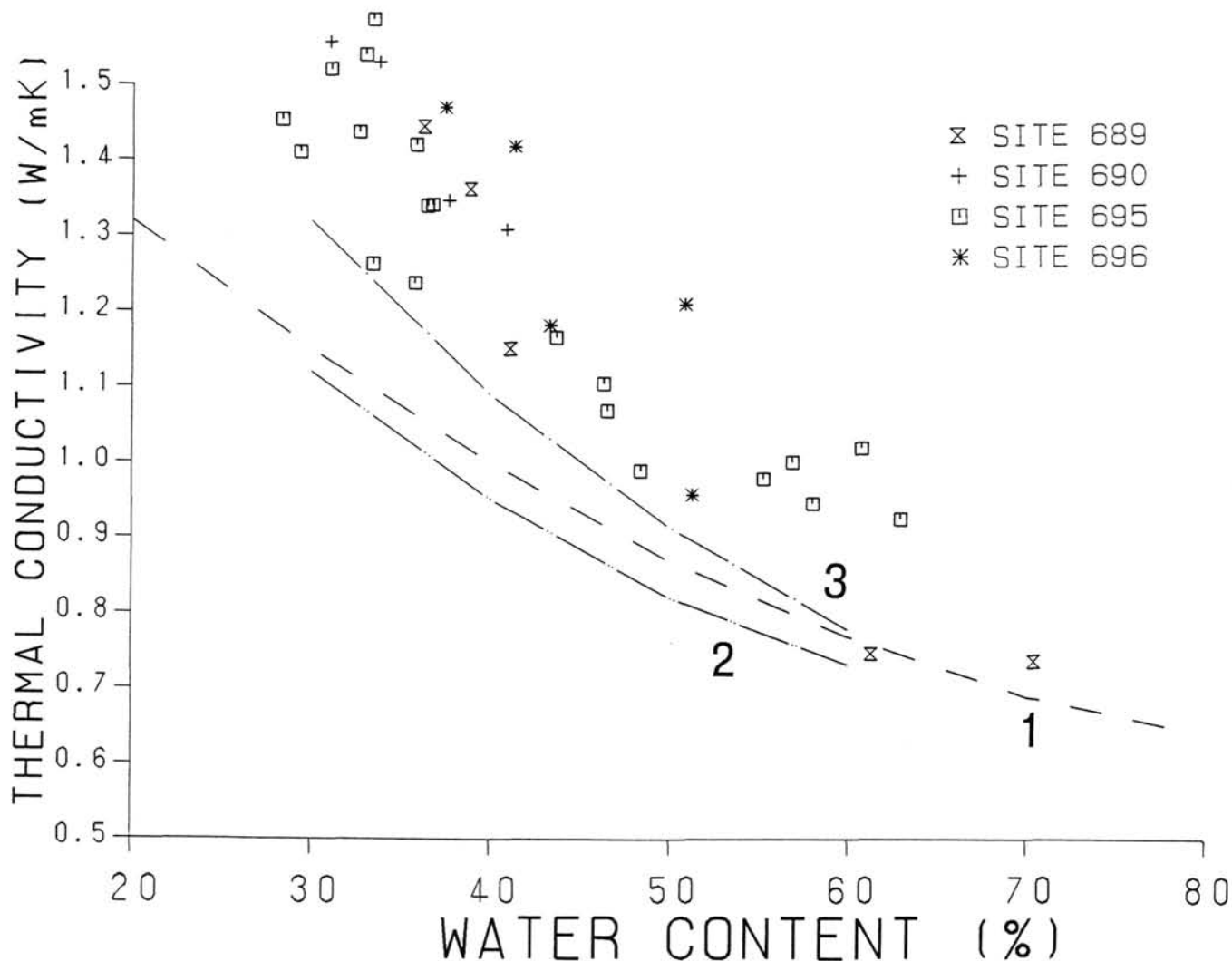


Figure 14. Observed thermal conductivity vs. measured water content. Dashed lines 1, 2, and 3 show the empirical relationships reported by Ratcliffe (1960), Bullard and Day (1961), and Lachenbruch and Marshall (1966), respectively.

Zlotnicki et al. (1980) to explain anomalous high heat flows in the Weddell Sea. Therefore, we can only conclude that the heat flow value at Site 690 is at least 45 mW/m^2 . For Site 689, we have one temperature vs. depth data point, and therefore no information on nonlinear temperature gradient. Simply multiplying the temperature gradient (98.5 mK/m) by the thermal conductivity ($0.87 \pm 0.19 \text{ W/m K}$, 13 data points), the heat flow is 85.7 mW/m^2 . However, at this stage, we can conclude that the heat flow at Site 689 is also at least 45 mW/m^2 .

Sites 695 and 696

At Site 695, one of the main objectives of heat flow measurements was to learn about the origin of a prominent BSR considered to represent the base of a gas hydrate, as mentioned before.

Figures 17 and 18 show results of all the temperature measurements and thermal conductivity data, respectively, from these two sites. Crosses show the observed temperature values just before pull-out, and arrows show the direction of temperature record change. Solid circles show the estimated true formation temperatures for Cores 113-695A-5H (41.2 mbsf) and -14H (118.2 mbsf). At Site 695, a temperature gradient was calculated as 54.7 mK/m by using values at these two depths.

Heat flow is defined as the product of a temperature gradient and thermal conductivity. We can calculate an uncorrected heat flow value at Site 695 of 62.3 mW/m^2 by using 54.7 mK/m for the temperature gradient and 1.14 W/m K for the thermal conductivity (between 41.2 and 118.2 mbsf, $1.14 \pm 0.16 \text{ W/m K}$, 16 data points).

The average thermal conductivities between 0 mbsf and 41.2 mbsf, and between 118.2 mbsf and 190.7 mbsf are $1.12 \pm 0.20 \text{ W/m K}$ (13 data points), and $1.08 \pm 0.10 \text{ W/m K}$ (15 data points), respectively. These results suggest that the thermal conductivity structure from 0 mbsf to 190.7 mbsf (Unit I; Barker, Kennett et al., 1988) is essentially constant. Therefore, we extrapolate the 54.7 mK/m gradient to this depth range. The average thermal conductivity value from 190.7 mbsf to 306.9 mbsf (Unit II, Barker, Kennett, et al., 1988) was 1.42 W/m K . If basal heat flux at this site, which is considered to be constant, is postulated as 62.3 mW/m^2 , then the 1.42 W/m K of thermal conductivity value produces a 43.7 mK/m temperature gradient in this depth range. The dashed line below 190.7 mbsf in Figure 17 was calculated in this manner. This temperature gradient yields 16.20°C at 312.7 mbsf. This estimated temperature profile is consistent with the actual measurement (Fig. 11).

Table 1. Thermal conductivity, porosity, wet weight water content, bulk density, grain density, and sonic velocity data for Holes 689B, 690B, 695A, and 696A.

Hole	Depth (mbsf)	Thermal conductivity (W/m K)	Water content (%)	Porosity (%)	Bulk density (g/cm ³)	Grain density (g/cm ³)	Velocity (m/s)
689B	8.6	0.738	70.5	84.1	1.22	1.99	1493
689B	18.0	0.748	61.3	82.1	1.37	2.52	1512
689B	65.8	1.152	41.1	63.1	1.57	2.50	1489
689B	75.4	1.446	36.2	61.1	1.73	2.76	1510
689B	85.0	1.364	38.8	63.9	1.69	2.72	1497
690B	93.0	1.310	40.9	66.0	1.65	2.72	1535
690B	102.7	1.349	37.6	67.6	1.84	2.63	
690B	112.4	1.531	33.7	59.5	1.81	2.76	1555
690B	122.4	1.558	31.0	58.6	1.94	2.77	1574
695A	3.7	1.422	35.8	62.0	1.77	2.91	1608
695A	62.8	1.541	32.9	59.7	1.85	2.90	1547
695A	65.8	1.341	36.4	61.0	1.72	2.70	1538
695A	72.4	0.948	58.0	80.0	1.41	2.63	1504
695A	75.0	1.106	46.3	70.2	1.55	2.61	1514
695A	102.7	1.167	43.7	70.6	1.66	2.88	1531
695A	110.9	1.070	46.5	70.8	1.56	2.55	1517
695A	112.3	0.980	55.3	78.9	1.46	2.63	1510
695A	120.6	0.927	62.9	82.8	1.35	2.26	1509
695A	122.1	1.003	56.9	79.6	1.43	2.57	
695A	130.3	1.022	60.7	78.2	1.32	2.15	1513
695A	169.2	0.990	48.4	73.2	1.55	2.72	1512
695A	246.8	1.412	29.3	54.9	1.92	2.70	
695A	249.8	1.522	31.0	55.8	1.84	2.72	1558
695A	256.5	1.343	36.7	62.2	1.74	2.72	
695A	259.5	1.239	35.7	62.2	1.78	2.63	
695A	266.2	1.264	33.4	60.4	1.85	2.83	
695A	267.7	1.439	32.6	59.6	1.87	2.78	
695A	297.7	1.455	28.3	53.5	1.94	2.69	
695A	304.8	1.588	33.3	58.9	1.81	2.77	
696A	12.4	1.183	43.3	68.9	1.63	2.65	1548
696A	46.3	0.959	51.3	73.2	1.46	2.44	1494
696A	52.6	1.212	50.9	76.5	1.54	2.64	
696A	55.6	1.420	41.3	67.1	1.66	2.71	
696A	72.0	1.472	37.4	62.6	1.71	2.63	1525

At this site, a prominent BSR at about 600 mbsf was postulated, before drilling, to be a gas hydrate. We observed thermal conductivity values greater than 2.0 W/m K below 300 mbsf. If we adopt a thermal conductivity below 300 mbsf of 2.2 W/m K (this is the maximum thermal conductivity value measured in the sedimentary rocks), the temperature at 600 mbsf would be about 26°C. This is a minimum temperature value. Therefore, it is difficult to believe that the inferred BSR at 600 mbsf is the base of a gas hydrate stability zone, because hydrates are not stable at such high temperatures (e.g., Shipley et al., 1979).

As to Site 696, a temperature gradient was tentatively calculated as 49 mK/m by using temperatures of 4.26°C at 69.6 mbsf and 7.88°C at 144.1 mbsf. Ten thermal conductivity measurements were made above 75.0 mbsf from Hole 696A samples and the averaged value is 1.24 ± 0.16 W/m K. From these values, the calculated (uncorrected) heat flow value at Site 696 is 60.8 mW/m².

Sites 695 and 696 have high sedimentation rates. The effect of rapid sedimentation on heat flow is discussed by many authors (e.g., Von Herzen and Uyeda, 1963; Langseth et al., 1980; Hutchison, 1985). Langseth et al. (1980) calculated the reduction of surface heat flow caused by sedimentation at a uniform rate, if a constant flux is provided at great depth. Hutchison (1985) discussed more complex histories of sedimentation. In this case, we used a simple sedimentation model. The mean sedimentation rate and duration at Sites 695 and 696 are 3.7×10^{-2} mm/y and 5×10^6 y, and 6.0×10^{-2} mm/y and 15×10^6 y, respectively (Barker, Kennett, et al., 1988). According to Langseth et al. (1980), estimated reduction factors at Sites 695 and 696 are

0.90 and 0.97 assuming the thermal diffusivity of 2×10^{-7} m²/s. Therefore, heat flow values at Sites 695 and 696, corrected for rapid sedimentation, are 69 and 63 mW/m², respectively. We consider that Sites 695 and 696 have essentially the same geothermal structure.

CONCLUSIONS

During Leg 113, heat flow was determined on Maud Rise (Sites 689 and 690) and on the southeast margin of the South Orkney microcontinent (Sites 695 and 696).

Regional magnetic anomaly data from around Maud Rise are sparse: a bight of Anomalies 33 and 34 is seen about 500 km northeast of Maud Rise, and M1 and older anomalies are found in both east and west (Bergh and Barrett, 1980; Barker et al., 1984). A Cretaceous age for Maud Rise, which these imply, is compatible with the Campanian age of basal sediments at Site 690 (Barker, Kennett, et al., 1988) and with a measured heat flow of 45 mW/m². This is a minimum heat flow value, however, and the errors associated with it are large. Contrary to expectations, it will not resolve the question of whether Maud Rise has a ridge crest or an off-axis origin.

Heat flow determinations at Sites 695 and 696 demonstrate that the prominent BSR beneath these sites cannot be the base of a gas hydrate stability zone. A widespread BSR in the Bering Sea, drilled during DSDP Leg 19 (Scholl and Creager, 1973) may have been caused by a diagenetic transition from Opal-A to opal-CT in diatomaceous sediments (Hammond and Gaither, 1983). A similar explanation may hold for the BSR on the South Orkney microcontinent.

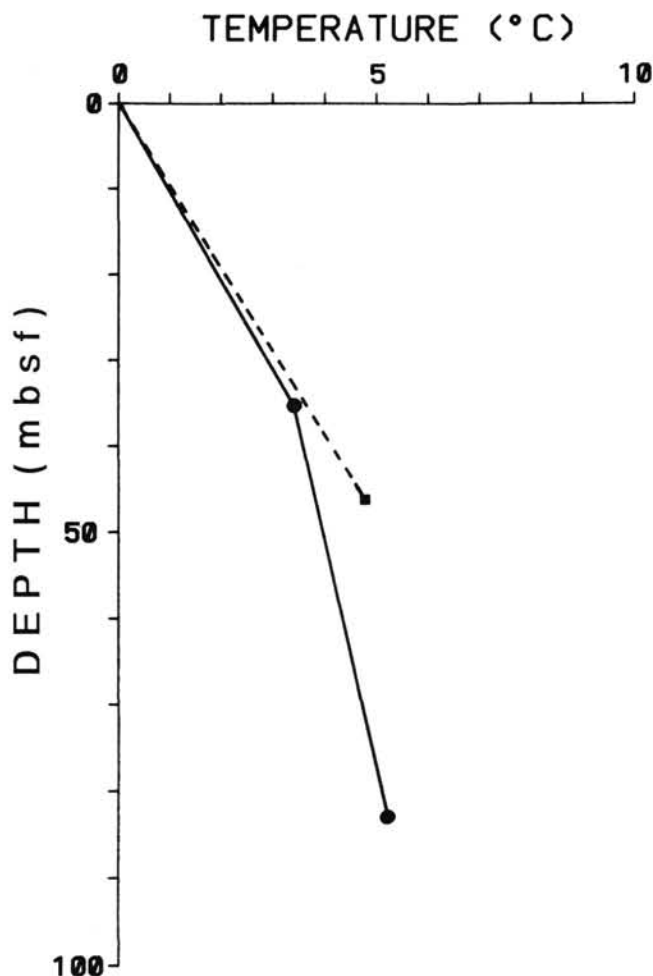


Figure 15. Temperature-depth profiles at Sites 689 (dashed line) and 690 (solid line).

ACKNOWLEDGMENTS

The author thanks Dr. Peter Barker for his useful suggestions and critical readings of this manuscript. My thanks are extended to Ms. Henrike M. Groschel-Becker, Mr. Jessy L. Jones, and Dr. William R. Bryant for their kind help with the onboard measurements.

REFERENCES

- Barker, P. F., Barber, P. L., and King, E. C., 1984. An early Miocene ridge crest-trench collision on the South Scotia Ridge near 36°W. *Tectonophysics*, 102:315-332.
- Barker, P. F., Kennett, J. P., et al., 1988. *Proc. ODP, Init. Repts.*, 113: College Station, TX (Ocean Drilling Program).
- Bergh, H. W., and Barrett, D. M., 1980. Agulhas Basin magnetic bight. *Nature*, 287:591-595.
- Bullard, E. C., and Day, A., 1961. The flow of heat through the floor of the Atlantic Ocean. *Geophys. J.*, 4 (spec. vol.): 282-292.
- Chapman, D. S., 1983. *International heat flow commission global heat flow density compilation*. World Data Center A.
- Dougherty, M. E., Von Herzen, R. P., and Barker, P. F., 1986. Anomalous heat flow from a Miocene ridge crest-trench collision, Antarctica. *Antarct. J. U. S.*, 21:151-153.
- Hammond, R. D., and Gaither, J. G., 1983. Anomalous seismic character—Bering Sea Shelf. *Geophysics*, 48:590-605.
- Horai, K., and Von Herzen, R. P., 1986. Measurement of heat flow on Leg 86 of the Deep Sea Drilling Project. In Heath, G. R., Burckle,

- L. H., et al., *Init. Repts. DSDP*, 86: Washington (U.S. Govt. Printing Office): 759-777.
- Hutchison, I., 1985. The effects of sedimentation and compaction on oceanic heat flow. *Geophys. J. R. Astr. Soc.*, 82:439-459.
- Kimura, K., 1982. Geological and geophysical survey in the Bellinghausen Basin, off Antarctica. *Antarct. Rec.*, 75:12-24.
- Lachenbruch, A. H., and Marshall, B. V., 1966. Heat flow through the Arctic Ocean floor: the Canada Basin-Alpha Rise boundary. *J. Geophys. Res.*, 71:1223-1248.
- Langseth, M. G., Hobart, M. A., and Horai, K., 1980. Heat flow in the Bering Sea. *J. Geophys. Res.*, 85:3740-3750.
- Lawver, L. A., Vedova, B. D., and Von Herzen, R. P., 1985. Heat-flow measurements in the Jane Basin, a back-arc basin, northern Weddell Sea. *Antarct. J. U. S.*, 19:87-88.
- Lister, C.R.B., 1977. Estimates for heat flow and deep rock properties based on boundary layer model. *Tectonophysics*, 41:157-171.
- Mizukoshi, I., Sunouchi, H., Saki, T., Sato, S., and Tanahashi, M., 1986. Preliminary report of geological and geophysical surveys off Amery Ice Shelf, East Antarctica. *Mem. Natl. Inst. Polar Res., Spec. Issue*, 43: 48-61.
- Morin, R. H., and Von Herzen, R. P., 1986. Geothermal measurements at Deep Sea Drilling Project Site 587. In Kennett, J. P., von der Borch, C. C., et al., *Init. Repts. DSDP*, 90: Washington (U.S. Govt. Printing Office), 1317-1324.
- Okuda, Y., Yamazaki, T., Sato, S., Saki, T., and Oikawa, N., 1983. Framework of the Weddell Basin inferred from the new geophysical and geological data. *Mem. Natl. Inst. Polar Res., Spec. Issue*, 28: 93-114.
- Parsons, B., and Sclater, J. G., 1977. An analysis of the variation of ocean floor bathymetry and heat flow with age. *J. Geophys. Res.*, 82: 803-827.
- Pudsey, C. J., Barker, P. F., and Hamilton, N., 1988. Weddell Sea abyssal sediments: A record of Antarctic bottom water flow. *Mar. Geol.*, 81:289-314.
- Ratcliffe, E. H., 1960. The thermal conductivities of ocean sediments. *J. Geophys. Res.*, 65:1535-1541.
- Saki, T., Tamura, Y., Tokuhashi, S., Kodato, T., Mizukoshi, I., and Amano, H., 1987. Preliminary report of geological and geophysical surveys off Queen Maud Land, East Antarctica. *Proc. NIPR Symp. Antarct. Geosci.*, 1:23-40.
- Sato, S., Asakura, N., Saki, T., Oikawa, N., and Kaneda, Y., 1984. Preliminary results of geological and geophysical surveys in the Ross Sea and in the Dumont D'Urville Sea, off Antarctica. *Mem. Natl. Inst. Polar Res., Spec. Issue*, 33:66-92.
- Scholl, D. W., and Creager, J. S., 1973. Geologic synthesis of Leg 19 (DSDP) results; far North Pacific, and Aleutian Ridge, and Bering Sea. In Sclater, J. G., Scholl, D. W., et al., *Init. Repts. DSDP*, 19: Washington (U.S. Govt. Printing Office), 897-913.
- Shipley, T. H., Houston, M. H., Buffler, R. T., Shaub, F. J., McMillen, K. J., Ladd, J. W., and Worzel, J. L., 1979. Seismic evidence for widespread possible gas hydrate horizons on continental slopes and rises. *Am. Assoc. Pet. Geol. Bull.*, 63:2204-2213.
- Tsumuraya, Y., Tanahashi, M., Saki, T., Machihara, T., and Asakura, N., 1985. Preliminary report of the marine geophysical and geological surveys off Wilks Land, Antarctica in 1983-1984. *Mem. Natl. Inst. Polar Res., Spec. Issue*, 37:48-62.
- Von Herzen, R. P., and Maxwell, A. E., 1959. The measurement of thermal conductivity of deep sea sediments by a needle-probe method. *J. Geophys. Res.*, 64:1557-1563.
- Von Herzen, R. P., and Uyeda, S., 1963. Heat flow through the Eastern Pacific Ocean floor. *J. Geophys. Res.*, 68(14):4219-4250.
- Yamaguchi, K., Tamura, Y., Mizukoshi, I., and Tsuru, T., 1988. Preliminary report of geophysical and geological surveys in Amundsen Sea, West Antarctica. *Proc. NIPR Symp. Antarct. Geosci.*, 2:55-67.
- Yokota, T., Kinoshita H., and Uyeda, S., 1980. New DSDP (Deep Sea Drilling Project) downhole temperature probe utilizing IC RAM (Memory) elements. *Bull. Earthquake Res. Inst.*, 55:75-88.
- Zlotnicki, V., Sclater, J. G., Norton, I. O., and Von Herzen, R. P., 1980. Heat flow through the floor of the Scotia, far south Atlantic and Weddell Seas. *Geophys. Res. Lett.*, 7 (4): 421-424.

Date of initial receipt: 17 December 1988

Date of acceptance: 19 October 1989

Ms 113B-183

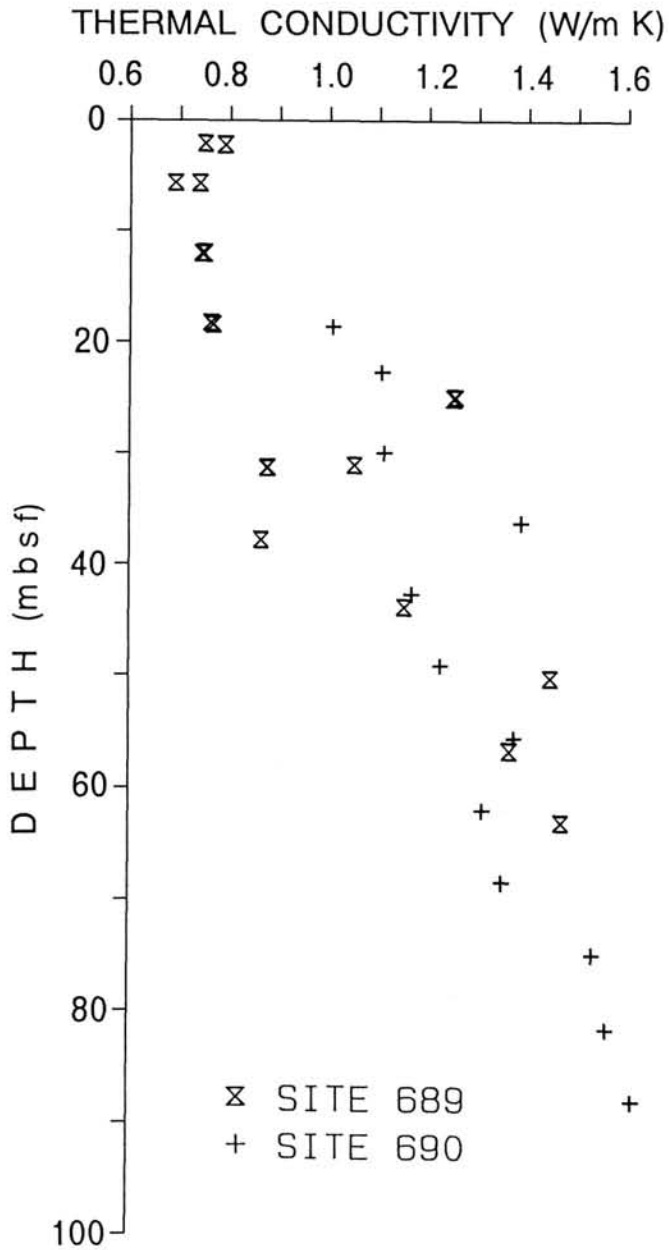


Figure 16. Thermal conductivity to 100 mbsf at Sites 689 and 690.

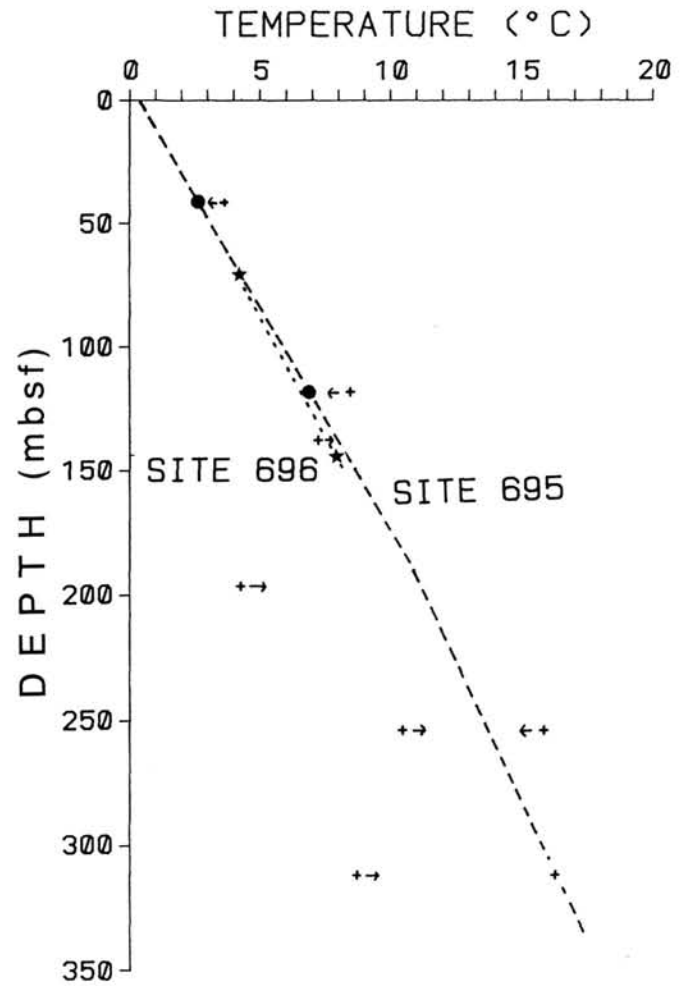


Figure 17. Observed temperature measurements just before pull-out (crosses) and estimated true formation temperatures (solid circles). Arrows show the temperature shifting directions. Dashed line shows the estimated temperature profile at Site 695. Dotted line with solid stars shows the estimated temperature profile at Site 696.

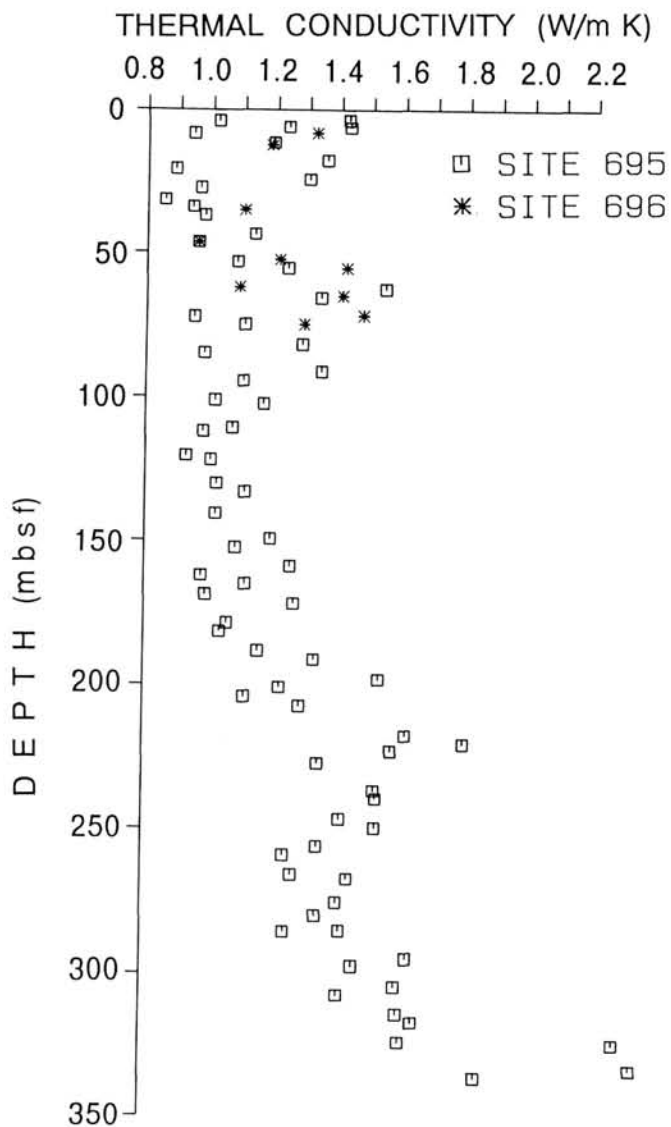


Figure 18. Measured thermal conductivity to 350 mbsf at Sites 695 and 696.